

Exploration of the nonsequential double-ionization process of a Mg atom with different delay time in few-cycle circularly polarized laser fields

Tong-Tong Xu, Shuai Ben, Tian Wang, Jun Zhang, Jing Guo,^{*} and Xue-Shen Liu[†]*Institute of Atomic and Molecular Physics, Jilin University, Changchun 130012, People's Republic of China*

(Received 28 May 2015; published 8 September 2015)

Using the three-dimensional classical ensemble method, we investigate the nonsequential double-ionization (NSDI) process of Mg in few-cycle circularly polarized laser fields. We demonstrate the time evolution of the distribution of the electron energy, the repulsion energy between double-ionized electrons, the distance between the nucleus and double-ionized electrons, and the momentum of double-ionized electrons. By analyzing these theoretical results, we find that a few-cycle pulse would allow a single recollision event. In addition, the correlated momentum distribution, the angular distribution between double-ionized electrons, and the ion momentum distribution with different delay time, which is the time interval between final double ionization and recollision, are also demonstrated and the results show that the delay time plays a key role in electron emission processes.

DOI: [10.1103/PhysRevA.92.033405](https://doi.org/10.1103/PhysRevA.92.033405)

PACS number(s): 32.80.Rm, 42.50.Hz, 42.65.Ky

I. INTRODUCTION

Nonsequential double ionization (NSDI) has been a hot topic in strong-field physics during the past two decades [1–3]. Since electron correlation plays an important role in the NSDI process, much of research on double ionization (DI) has been focused on electron correlations [4], including angular correlation [5–7] and recollision [8–10], etc. Generally, for most atoms, NSDI always occurs in a linearly polarized laser field, but for Mg this is not the case. Thus, the NSDI process of Mg observed in circularly polarized (CP) fields [11] provides a method for studying electron-electron correlation for deeper understanding of strong-field processes.

In the recollision picture, the first released electron has traveled out from the core, and then it is driven back by the laser field and shares its kinetic energy with the second electron [12]. A number of theoretical studies and experimental works prove that ionized electron pairs have been emitted in the same directions after recollision [13–17]. However, experiments with noble gas atoms [18,19] using cold target recoil ion momentum spectroscopy find a great number of ionized electron pairs have been emitted in opposite directions as well. These features provide strong evidence that both correlation and anticorrelation behaviors contribute to the NSDI process. More interestingly, Liu *et al.* [20] also demonstrated experimentally that at the laser intensity below the recollision threshold the correlated electron pairs from NSDI of atoms drift out by opposite emissions; this is called the anticorrelated phenomenon. Many theoretical studies show that the anticorrelation behavior is related to the delayed emission of the second electron after recollision [21–24]. Most of earlier NSDI experiments have been implemented by using many-cycle laser pulses. However, multiple recollisions contribute to the NSDI process, which could make it difficult to understand the detailed recollision dynamics clearly [25]. By using the few-cycle laser pulse, we can achieve a single recollision event in NSDI process,

which may help us understand the electron correlation more clearly.

In this paper, we use the classical ensemble method to investigate the NSDI processes of three-dimensional Mg in few-cycle CP laser fields. The ionization probability of Mg as a function of laser intensity is calculated. We demonstrate that a few-cycle pulse would allow a single recollision event. Moreover, we investigate the correlated momentum distribution, the angular distribution between double-ionized electrons, and the ion momentum distribution with different delay time and the results show that the delay time plays a key role in the electron emission process.

II. THEORETICAL MODEL AND NUMERICAL METHOD

We explore the ionization dynamics of Mg in few-cycle CP laser fields by using the classical ensemble method [26]. The model of Mg has been used before [7,9,10]. The three-dimensional (3D) classical Hamiltonian of Mg is given by (atomic units are used throughout unless otherwise stated)

$$H(\mathbf{r}_1, \mathbf{r}_2; \mathbf{P}_1, \mathbf{P}_2; t) = \mathcal{T}(p) + \mathcal{V}(q, t). \quad (1)$$

In the above equation, $\mathcal{T}(p)$ is the kinetic energy and $\mathcal{V}(q, t)$ is the potential energy, which can be given by

$$\mathcal{T}(p) = \frac{\mathbf{P}_1^2}{2} + \frac{\mathbf{P}_2^2}{2}, \quad (2)$$

$$\mathcal{V}(q, t) = - \sum_{i=1}^2 \frac{2}{|\mathbf{r}_i|} + \frac{1}{|\mathbf{r}_1 - \mathbf{r}_2|} + (\mathbf{r}_1 + \mathbf{r}_2)E(t), \quad (3)$$

where $q = (\mathbf{r}_1, \mathbf{r}_2)$ is the label of the positions of the two electrons and $p = (\mathbf{P}_1, \mathbf{P}_2)$ is the corresponding conjugate momentum. The CP electric fields can be chosen as $E(t) = E_0 f(t)[\hat{x} \sin(\omega t + \varphi) + \hat{y} \cos(\omega t + \varphi)]$ with frequency $\omega = 0.061$ a.u. (750 nm in wavelength); $f(t) = \sin^2(\pi t/\tau)$ is the envelope pulse; the full duration is four optical cycles (o.c.); E_0 is the peak intensity, and φ is the carrier-envelope phases

^{*}gjing@jlu.edu.cn[†]liuxs@jlu.edu.cn

(CEPs). We use the soft core potential

$$\mathcal{V}(q) = -\sum_{i=1}^2 \frac{2}{\sqrt{|\mathbf{r}_i|^2 + a^2}} + \frac{1}{\sqrt{(\mathbf{r}_1 - \mathbf{r}_2)^2 + b^2}} \quad (4)$$

with the soft core parameters $a = 3.0$ and $b = 0.05$ to avoid the autoionization states and remove the singularity of the Coulomb potentials. The first term on the right represents the ion-electron interactions and the second term on the right represents the electron-electron interactions, respectively.

The symplectic method is suitable for long-time many-step calculations and preserves the symplectic structure of the system. By solving the Hamiltonian canonical equations numerically with the symplectic method, we can obtain the time evolutions of electron positions and the corresponding momentum. The Hamiltonian of the system (1) contains separately the p and the q in $\mathcal{T}(p)$ and $\mathcal{V}(q,t)$, which is a separable Hamiltonian system. We may use an explicit symplectic scheme to solve the corresponding Hamiltonian canonical equation in order to obtain the classical trajectories of Mg in an intense laser field. For instance, we can solve the Hamiltonian canonical equation by the four-stage fourth-order explicit symplectic scheme [27].

In our calculation, the initial condition has the same energy, which approximately equals the sum of the first and second ionization energies [28], which is about -0.8 a.u. [29]. Once the initial ensemble is confirmed, the laser field is turned on and all trajectories in the intense laser field evolve. We can work with large number ensembles of classical electron pairs in a statistical manner. Here, we define an electron to be ionized if its energy is greater than zero at the end of the laser pulse.

III. RESULTS AND DISCUSSION

Figure 1 presents the DI probability of Mg as a function of laser intensity in CP laser fields with a wavelength of

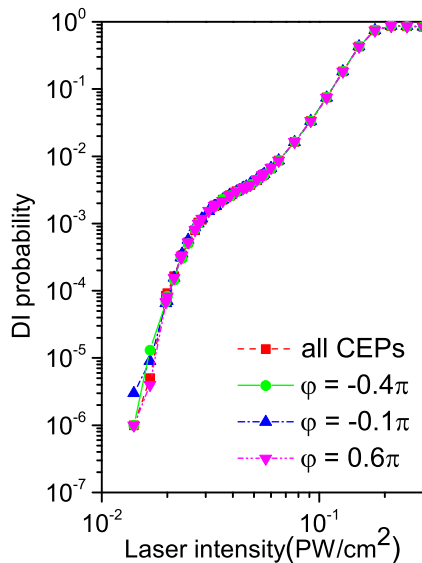


FIG. 1. (Color online) Double-ionization probability of Mg as a function of the laser intensity in CP laser fields with different CEPs. The laser wavelength is 750 nm.

750 nm and different CEPs. We can see that a “knee” structure occurs in Fig. 1, which is in agreement with the corresponding experimental results and numerical calculations [10,11]. We can also see that the knee structure is unchanged for different CEPs, which means that the NSDI probability of Mg is not influenced by CEPs. Besides, with the laser parameters we used in this paper, the knee structure occurs in the range of $0.03 \sim 0.07$ PW/cm².

In order to further explore or understand the mechanism of NSDI of Mg in few-cycle CP laser fields with all CEPs, we demonstrate the time evolution of the electron energy ($E_i = \frac{|\mathbf{p}_i|^2}{2} - \frac{2}{\sqrt{|\mathbf{r}_i|^2 + a^2}} + \frac{1}{\sqrt{|\mathbf{r}_1 - \mathbf{r}_2|^2 + b^2}}$, $i = 1, 2$) distribution [30], the repulsion energy ($E_p = \frac{1}{\sqrt{|\mathbf{r}_1 - \mathbf{r}_2|^2 + b^2}}$) distribution between two electrons, the distance distribution between the nucleus and double-ionized electrons, and the momentum distribution of double-ionized electrons at the laser peak intensity $I = 0.04$ PW/cm² as shown in Fig. 2.

Figure 2(a) shows the time evolution of the electron energy distribution of double-ionized electrons. We can see that the electron energy oscillates in the range of $-0.5 \sim -0.13$ a.u. After a period of time, the distribution splits into two branches. One of them emerges from the positive-energy region while the other drops to a lower negative-energy region, which shows that single ionization occurs after the first optical cycle. The ionized electron returns to the core during the second optical cycle (the energy become negative) and collides with the second electron, which corresponds to a recollision process. By the third optical cycle, the two branches turn into one branch and emerge at the positive-energy region, which shows that the double ionization is completed.

Figure 2(b) shows the repulsion energy distribution between two electrons as functions of time. Similarly, first of all the repulsion energy also presents the oscillation in the range of $0.15 \sim 0.4$ a.u., which lasts 0.67 o.c. Then the repulsion energy decreases rapidly, which shows the single ionization occurs after the first optical cycle. The repulsion energy around the second optical cycle is as high as that around 0.67 o.c., which shows the ionized electron returns to the core. The above phenomenon is in accordance with that illustrated in Fig. 2(a).

Figure 2(c) shows the time evolution of the distance distribution between the nucleus and double-ionized electrons. There is a peak value at about 1.4 o.c., which shows the single ionization occurs. Then the distance decreases rapidly up to about 0 a.u. around 2 o.c. and then increases rapidly until the end of the pulse. Figure 2(c) also illustrates that a single recollision happens.

Figure 2(d) shows the time evolution of the momentum distribution of double-ionized electrons. Similarly, first of all the momentum also presents the oscillation in the range of $0 \sim 0.35$ a.u. which lasts 0.67 o.c. Due to the energy sharing and subsequent electric field effect, one of the ionized electrons slows down quickly and the other speeds up after recollision.

Thus we can conclude from Fig. 2 that there is a single recollision event in the NSDI process in a few-cycle CP laser field at the laser peak intensity $I = 0.04$ PW/cm². Because multiple recollisions contribute to the NSDI process in multicycle lasers, it is difficult to understand the detailed

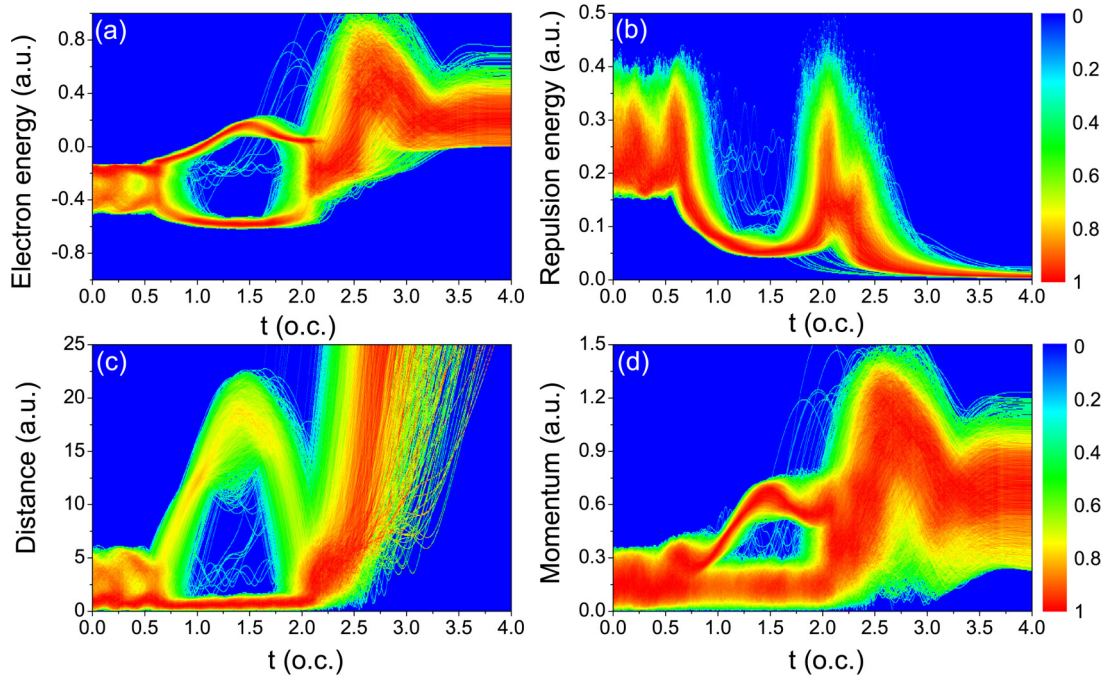


FIG. 2. (Color online) Time evolution of (a) the electron energy distribution, (b) the repulsion energy distribution between two electrons, (c) the distance distribution between the nucleus and double-ionized electrons, and (d) the momentum distribution of double-ionized electrons in the CP laser fields with a wavelength of 750 nm and a laser peak intensity of $I = 0.04$ PW/cm².

recollision dynamics clearly [25]. By using the few-cycle laser pulse, we can achieve a single recollision event in the NSDI process, which may help us understand the electron correlation more clearly.

The time interval between recollision and final double ionization is defined as the delay time (t_D). Figure 3(a) shows the counts of NSDI trajectories versus the delay time. We can see that the range of the delay time is distributed from 0 to 1 o.c. and the counts of NSDI trajectories are the biggest at about 0.4 o.c. We discuss the delay time at about 0.5 o.c. for clarity and without loss of generality. Figure 3(b) shows the map of the double-ionization time (t_{DI}) versus the recollision time (t_r). It clearly shows that NSDI events are mainly continuously clustered in a single region, the

recollision time is distributed in the range of $1.75 \sim 2.2$ o.c., and the double ionization occurs after 2.15 o.c. We know that the whole range of the delay time is from 0 to 1 o.c., which is shown in Fig. 3(a). We give the delay time $t_D = t_{DI} - t_r = 0.5$ o.c., which is indicated by the white dashed line in Fig. 3(b). We point out that the lower region of the white dashed line represents the short delay time ($t_D < 0.5$ o.c.), and the upper region of the white dashed line represents the long delay time ($t_D > 0.5$ o.c.). In Ref [25], it was found that NSDI events of Ar mainly cluster two regions in the linearly polarized laser fields with a wavelength of 750 nm and a laser intensity of $I = 0.3$ PW/cm², which is different from Mg in the CP laser fields with a wavelength of 750 nm and a laser peak intensity of $I = 0.04$ PW/cm².

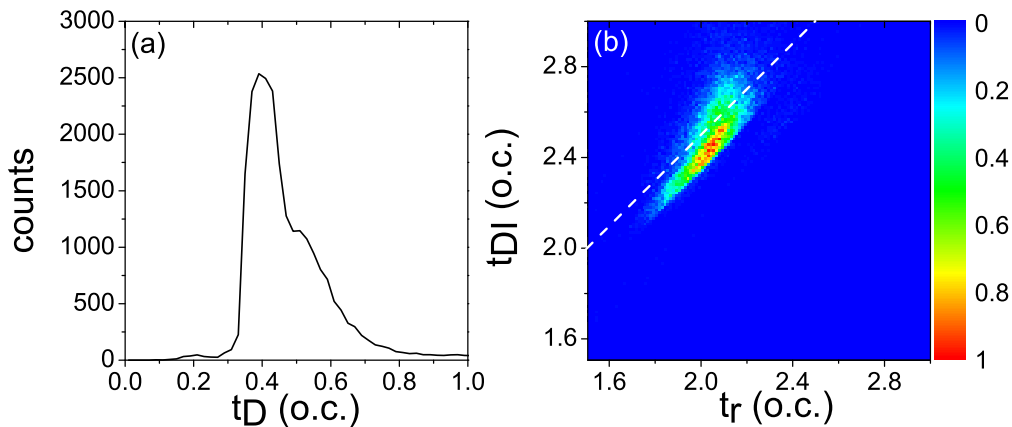


FIG. 3. (Color online) (a) Counts of NSDI trajectories versus the delay time in CP laser fields at a laser peak intensity of $I = 0.04$ PW/cm². (b) The map of the double-ionization time (t_{DI}) versus the recollision time (t_r) in CP laser fields. The white dashed line indicates the delay time $t_D = t_{DI} - t_r = 0.5$ o.c.

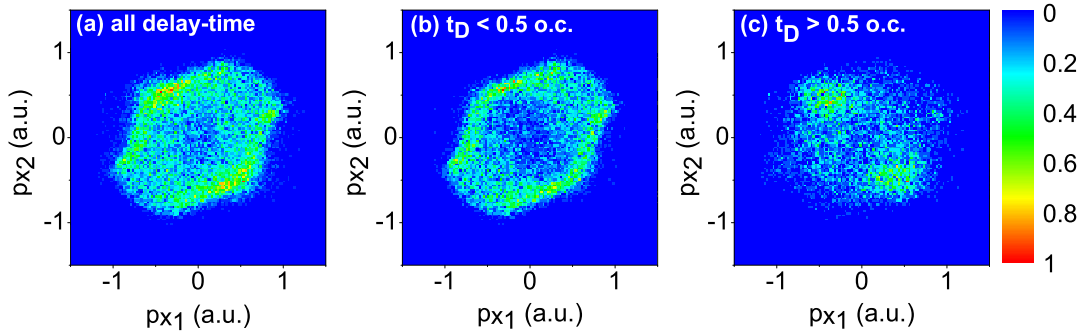


FIG. 4. (Color online) The correlated momentum distribution of Mg at the end of the laser pulse with different delay time in CP laser fields at a laser peak intensity of $I = 0.04 \text{ PW/cm}^2$: (a) all delay time, (b) $t_D < 0.5 \text{ o.c.}$, and (c) $t_D > 0.5 \text{ o.c.}$

The correlated momentum distribution at the end of the laser pulse is shown in Fig. 4. Figure 4(a) shows that the electron momentum distributes in four quadrants at all delay times. In order to explore the difference in electron correlation, we show the correlated momentum distribution with a short delay time and a long delay time in Figs. 4(b) and 4(c), respectively. For $t_D < 0.5 \text{ o.c.}$ [as shown in Fig. 4(b)], most of the electron momentum is mainly distributed in the first and third quadrants compared with that shown in Fig. 4(c) ($t_D > 0.5 \text{ o.c.}$), which shows the correlation between two electrons is predominant. However, for $t_D > 0.5 \text{ o.c.}$ [as shown in Fig. 4(c)], the electron momentum is mainly distributed in the second and fourth quadrants, indicating that the anticorrelation between two electrons is predominant.

For a short delay time ($t_D < 0.5 \text{ o.c.}$), the returning electron collides with the other electron strongly and transfers enough energy to it during the recollision, the other electron obtains a little energy from the electronic field, and then the double ionization is completed. Thus, the double ionization with a short delay time ($t_D < 0.5 \text{ o.c.}$) following “hard-hit” recollision leads to the same emission of two electrons (correlated phenomenon) [21]. On the contrary, if the returning electron collides with the other electron not so strongly, the other electron needs to obtain more energy from the electronic field

in a long delay time ($t_D > 0.5 \text{ o.c.}$), which leads to the opposite emission of two electrons (anticorrelated phenomenon). This is similar to that indicated in Ref. [21], which illustrated that the two electrons are emitted into opposite directions for an increasing time interval between recollision and double ionization (delay time).

We present the angular distribution between double-ionized electrons at the end of the laser pulse in CP laser fields in Fig. 5. The angle between double-ionized electrons at the end of the laser pulse is defined as θ . For $t_D < 0.5 \text{ o.c.}$ [as shown in Fig. 5(a)], the angle θ is mainly distributed at $60^\circ \sim 90^\circ$ and $270^\circ \sim 300^\circ$, which means that the two electrons are more likely to be emitted into the same direction. For $t_D > 0.5 \text{ o.c.}$ [as shown in Fig. 5(b)], the angle θ is distributed at $90^\circ \sim 270^\circ$ and the two electrons have more probability to be emitted with $150^\circ \sim 210^\circ$, which means that the two electrons are more likely to be emitted in opposite directions.

Finally, the ion momentum distribution at the end of the laser pulse is presented in Fig. 6, which can reflect the correlation between the two electrons [6]. Figure 6(a) shows that the ion momentum distribution at all delay times presents a circular structure. The momentum of the ion is larger if the two electrons are emitted in the same direction than that if the two electrons are emitted in opposite directions [6].

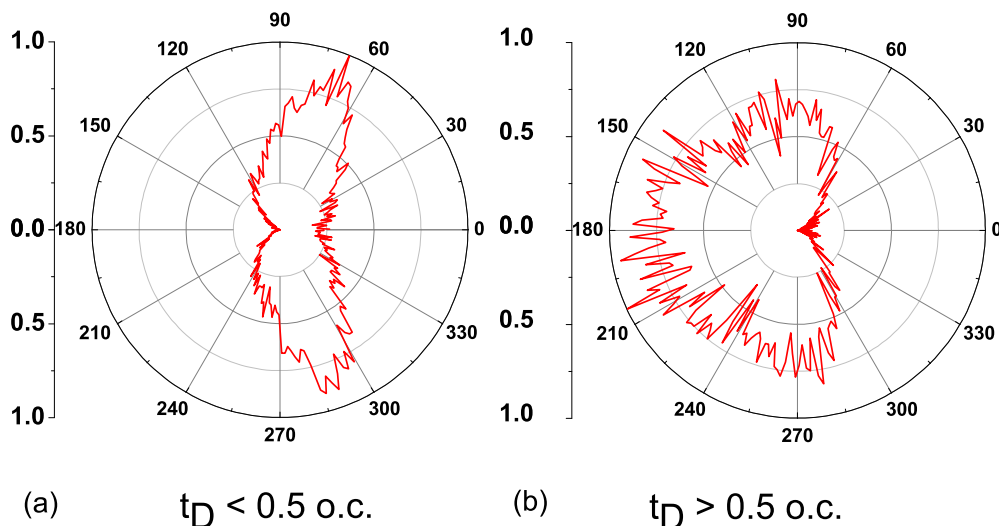


FIG. 5. (Color online) The angular distribution between double-ionized electrons with different delay time at the end of laser pulse in CP laser fields at a laser peak intensity of $I = 0.04 \text{ PW/cm}^2$: (a) $t_D < 0.5 \text{ o.c.}$ and (b) $t_D > 0.5 \text{ o.c.}$

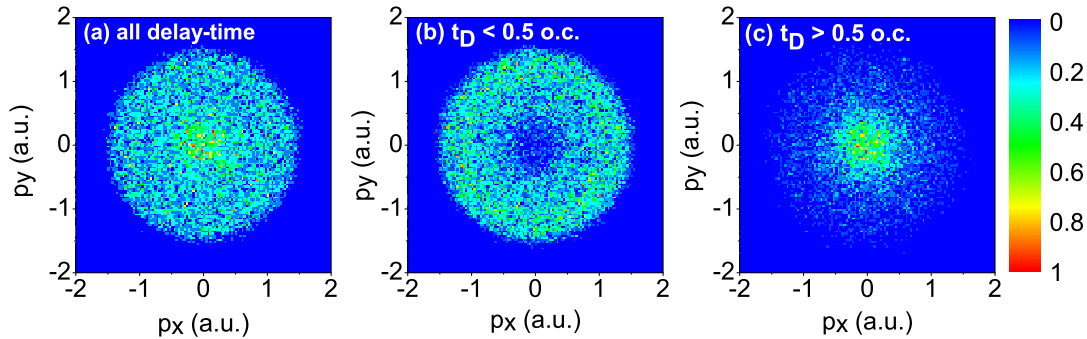


FIG. 6. (Color online) Ion momentum distributions at the end of the laser pulse with different delay time in the CP laser fields at a laser peak intensity of $I = 0.04 \text{ PW/cm}^2$: (a) all delay time, (b) $t_D < 0.5 \text{ o.c.}$, and (c) $t_D > 0.5 \text{ o.c.}$

For $t_D < 0.5 \text{ o.c.}$, Fig. 6(b) shows that the ion momentum distribution around the origin is sparse, but the ion momentum away from the origin is more populated, which illustrates that the two electrons are more likely to be emitted in the same direction. However, for $t_D > 0.5 \text{ o.c.}$, Fig. 6(c) shows that the ion momentum distribution around the origin is more populated, but the ion momentum distribution away from the origin is sparse, which illustrates that the two electrons are more likely to be emitted in opposite directions. The mechanism demonstrated in Fig. 6 is in accordance with that illustrated in Figs. 4 and 5.

IV. CONCLUSIONS

In summary, we use the 3D classical ensemble method to investigate the NSDI processes of Mg in few-cycle CP laser fields. By analyzing the time evolution of the distribution of the electron energy, the repulsion energy between double ionized electrons, the distance between the nucleus and double-ionized electrons, and the momentum of double-ionized electrons, we can sufficiently illustrate that a single recollision event occurs in CP laser fields with the laser

parameters we used. We illustrate that the delay time plays a key role in the electron emission process by analyzing the correlated momentum distribution and the ion momentum distribution. For $t_D < 0.5 \text{ o.c.}$, the ion momentum distribution around the origin is sparse, but the ion momentum away from the origin is more populated, which means that the correlation between two electrons is predominant. However, for $t_D > 0.5 \text{ o.c.}$, the ion momentum distribution around the origin is more populated, while the ion momentum distribution away from the origin is sparse, which indicates that the anticorrelation between two electrons is predominant. In addition, we also investigate the angular distribution between the double-ionized electrons at the end of the laser pulse with different delay time, and the results show that the double-ionized electrons are more likely to be ejected in opposite directions for a long delay time during the NSDI process in CP laser fields.

ACKNOWLEDGMENTS

We thank Prof. Xue-Bin Bian for his critical reading of the manuscript. This work was supported by the National Natural Science Foundation of China (Grants No. 11271158, No. 11174108, and No. 61575077).

-
- [1] D. N. Fittinghoff, P. R. Bolton, B. Chang, and K. C. Kulander, *Phys. Rev. Lett.* **69**, 2642 (1992).
 - [2] B. Walker, B. Sheehy, L. F. DiMauro, P. Agostini, K. J. Schafer, and K. C. Kulander, *Phys. Rev. Lett.* **73**, 1227 (1994).
 - [3] H. Y. Li, B. B. Wang, J. Chen, H. B. Jiang, X. F. Li, J. Liu, Q. H. Gong, Z. C. Yan, and P. Fu, *Phys. Rev. A* **76**, 033405 (2007).
 - [4] W. Becker, X. J. Liu, P. J. Ho, and J. H. Eberly, *Rev. Mod. Phys.* **84**, 1011 (2012).
 - [5] A. Fleischer, H. J. Wörner, L. Arissian, L. R. Liu, M. Meckel, A. Rippert, R. Dörner, D. M. Villeneuve, P. B. Corkum, and A. Staudte, *Phys. Rev. Lett.* **107**, 113003 (2011).
 - [6] X. Wang, J. Tian, and J. H. Eberly, *Phys. Rev. Lett.* **110**, 073001 (2013).
 - [7] J. Guo, T. Wang, X. S. Liu, and J. Z. Sun, *Laser Phys.* **23**, 055303 (2013).
 - [8] X. L. Hao, G. Q. Wang, X. Y. Jia, W. D. Li, J. Liu, and J. Chen, *Phys. Rev. A* **80**, 023408 (2009).
 - [9] L. B. Fu, G. G. Xin, D. F. Ye, and J. Liu, *Phys. Rev. Lett.* **108**, 103601 (2012).
 - [10] F. Mauger, C. Chandre, and T. Uzer, *Phys. Rev. Lett.* **105**, 083002 (2010).
 - [11] G. D. Gillen, M. A. Walker, and L. D. Van Woerkom, *Phys. Rev. A* **64**, 043413 (2001).
 - [12] P. B. Corkum, *Phys. Rev. Lett.* **71**, 1994 (1993).
 - [13] S. P. Goreslavskii, S. V. Popruzhenko, R. Kopold, and W. Becker, *Phys. Rev. A* **64**, 053402 (2001).
 - [14] A. Becker and F. H. M. Faisal, *Phys. Rev. Lett.* **89**, 193003 (2002).
 - [15] L. B. Fu, J. Liu, and S. G. Chen, *Phys. Rev. A* **65**, 021406 (2002).
 - [16] J. Chen and C. H. Nam, *Phys. Rev. A* **66**, 053415 (2002).
 - [17] Th. Weber, H. Giessen, M. Weckenbrock, G. Urbasch, A. Staudte, L. Spielberger, O. Jagutzki, V. Mergel, M. Vollmer, and R. Dörner, *Nature (London)* **405**, 658 (2000).
 - [18] M. Weckenbrock, D. Zeidler, A. Staudte, Th. W. eber, M. Schöffler, M. Meckel, S. Kammer, M. Smolarski, O. Jagutzki, V. R. Bhardwaj, D. M. Rayner, D. M. Villeneuve, P. B. Corkum, and R. Dörner, *Phys. Rev. Lett.* **92**, 213002 (2004).

- [19] B. Feuerstein, R. Moshhammer, D. Fischer *et al.*, *Phys. Rev. Lett.* **87**, 043003 (2001).
- [20] Y. Liu, S. Tschuch, A. Rudenko, M. Dürr, M. Siegel, U. Morgner, R. Moshhammer, and J. Ullrich, *Phys. Rev. Lett.* **101**, 053001 (2008).
- [21] S. L. Haan, L. Breen, A. Karim, and J. H. Eberly, *Phys. Rev. Lett.* **97**, 103008 (2006).
- [22] S. L. Haan, Z. S. Smith, K. N. Shomsky, and P. W. Plantinga, *J. Phys. B* **41**, 211002 (2008).
- [23] D. F. Ye and J. Liu, *Phys. Rev. A* **81**, 043402 (2010).
- [24] D. F. Ye, X. Liu, and J. Liu, *Phys. Rev. Lett.* **101**, 233003 (2008).
- [25] C. Huang, Y. M. Zhou, Q. B. Zhang, and P. X. Lu, *Opt. Express* **21**, 11382 (2013).
- [26] R. Panfili, J. H. Eberly, and S. L. Haan, *Opt. Express* **8**, 431 (2001).
- [27] X.-S. Liu, Y.-Y. Qi, J.-F. He, and P.-Z. Ding, *Commun. Comput. Phys.* **2**, 1 (2007).
- [28] J. Guo, X.-S. Liu, and Shih-I Chu, *Phys. Rev. A* **88**, 023405 (2013).
- [29] X. Wang, Theory of Strong-Field Atomic Ionization for Elliptical or Circular Polarization, Ph.D. thesis, University of Rochester, Rochester, NY, 2013.
- [30] T. Wang, X. L. Ge, J. Guo, and X. S. Liu, *Phys. Rev. A* **90**, 033420 (2014).